

Exclusive vector meson production in electron-ion collisions

V.P. Gonçalves¹, M.S. Kugeratski², M.V.T. Machado³ and F.S. Navarra²

¹ *Instituto de Física e Matemática,
Universidade Federal de Pelotas
Caixa Postal 354, CEP 96010-090, Pelotas, RS, Brazil*

² *Instituto de Física, Universidade de São Paulo,
C.P. 66318, 05315-970 São Paulo, SP, Brazil*

³ *Centro de Ciências Exatas e Tecnológicas,
Universidade Federal do Pampa
Campus de Bagé, Rua Carlos Barbosa. CEP 96400-970. Bagé, RS, Brazil*

We calculate the nuclear cross section for coherent and incoherent vector meson production within the QCD color dipole picture, including saturation effects. Theoretical estimates for scattering on both light and heavy nuclei are given over a wide range of energy.

PACS numbers: 12.38.-t, 24.85.+p, 25.30.-c

Keywords: Quantum Chromodynamics, Vector Meson Production, Saturation effects.

I. INTRODUCTION

One of the main theoretical expectations for the high energy regime of Quantum Chromodynamics (QCD) is the saturation of the parton densities in hadrons and nuclei at small values of the Bjorken- x variable and the formation of a Color Glass Condensate (CGC). This is one of the main topics of hadron physics to be explored in the new accelerators, such as the LHC and possibly the future electron-ion collider. The search for signatures of the CGC has been subject of an active research (for recent reviews see, e.g. [1]), with the experimental data being successfully described by phenomenological models based on saturation physics [2, 3, 4, 5, 6, 7]. However, more definite conclusions are not yet possible. In order to discriminate between these different approaches and test the CGC physics, it would be very important to consider an alternative search. To this purpose, the future electron-ion colliders offer a promising opportunity [8, 9].

In a series of papers [10, 11, 12, 13] we investigated the prospects of observing the CGC in a future electron-ion collider (For related studies see Refs. [14, 15, 16]). As it has been already emphasized in these papers, the advantage of using nuclear targets is that the saturation scale Q_s is much larger and this is crucial for the observation of most of the CGC effects. After these studies our conclusion was that it is very difficult to disentangle CGC effects from the standard linear QCD looking only at the nuclear inclusive observables, such as the nuclear structure functions F_2^A , $F_2^{c,A}$ and F_L^A . On the other hand, the study of diffractive observables was shown to be promising, as demonstrated in Refs. [11, 13]. In particular, in [13] we found out that the saturation models are able to describe the current data on the nuclear structure function F_2^A and predict that the contribution of diffractive events to the total cross section should be of $\approx 20\%$ at large A and small Q^2 . In the asymptotic limit of very high energies diffractive events are expected to form half of the total cross section, with the other half being formed by all inelastic processes [17]. This observation motivates a more detailed study of diffractive processes. In particular, we can expect that the study of exclusive processes, such as diffractive vector meson production, can be useful to determine the QCD dynamics at high energies. It is important to emphasize that the experimental HERA data on vector meson production in ep processes are successfully described by the phenomenological saturation models (See, e.g., [5, 18, 19, 20, 21, 22]). In contrast, very little is known about vector meson production off nuclei at high energies. Exclusive vector meson production in eA interactions can be classified as coherent or incoherent. If the reaction leaves the target intact, the process is usually called coherent. Otherwise it is called incoherent. These two types of diffractive hadron production were studied recently in Refs. [23, 24, 25, 26, 27] using the CGC formalism. The main conclusion of these works is that coherent production can serve as a sensitive probe of the high energy dynamics of nuclear matter, while incoherent production measures the fluctuations of the nuclear color fields. These findings are an additional motivation for our study of nuclear vector meson production. We focus our analysis on exclusive vector meson production by real and virtual photons, which may help us to understand several physical issues, besides saturation effects. Among these we find, for example, the transition from the soft dynamics (at low virtualities of the photon Q^2) to the hard perturbative

regime at high Q^2 and the relative weights of coherent and incoherent interactions between the projectile and the target nucleus.

In this paper we calculate the coherent and incoherent production cross sections of vector meson production using the dipole approach and a nuclear saturation model based on CGC physics. The main input for our calculation is the dipole-target cross section, $\sigma_{dip}^{\text{target}} = \sigma_{dip}(x, \mathbf{r})$, which is determined by the QCD dynamics at small x . In the eikonal approximation it is given by:

$$\sigma_{dip}(x, \mathbf{r}) = 2 \int d^2\mathbf{b} \mathcal{N}(x, \mathbf{r}, \mathbf{b}) \quad (1)$$

where $\mathcal{N}(x, \mathbf{r}, \mathbf{b})$ is the forward dipole-target scattering amplitude for a dipole with size \mathbf{r} and impact parameter \mathbf{b} which encodes all the information about the hadronic scattering, and thus about the non-linear and quantum effects in the hadron wave function (see e.g. [1]). It can be obtained by solving the BK (JIMWLK) evolution equation in the rapidity $Y \equiv \ln(1/x)$. Many groups have studied the numerical solution of the BK equation, but several improvements are still necessary before using the solution in the calculation of observables. In particular, one needs to include the next-to-leading order corrections into the evolution equation and perform a global analysis of all small x data. It is a program in progress (for recent results see [28, 29]). In the meantime it is necessary to use phenomenological models for \mathcal{N} which capture the most essential properties of the solution. Following [13] we will use in our calculations the model proposed in Ref. [30], which describes the current scarce experimental data on the nuclear structure function as well as includes the impact parameter dependence in the dipole nucleus cross section. In this model the forward dipole-nucleus amplitude is given by

$$\mathcal{N}^A(x, \mathbf{r}, \mathbf{b}) = 1 - \exp \left[-\frac{1}{2} \sigma_{dp}(x, \mathbf{r}^2) T_A(\mathbf{b}) \right], \quad (2)$$

where σ_{dp} is the dipole-proton cross section and $T_A(\mathbf{b})$ is the nuclear profile function, which is obtained from a 3-parameter Fermi distribution for the nuclear density normalized to A (for details see, e.g., Ref. [31]). The above equation, based on the Glauber-Gribov formalism [32], sums up all the multiple elastic rescattering diagrams of the $q\bar{q}$ pair and is justified for large coherence length, where the transverse separation r of partons in the multiparton Fock state of the photon becomes a conserved quantity, *i.e.* the size of the pair r becomes eigenvalue of the scattering matrix. It is important to emphasize that for very small values of x , other diagrams beyond the multiple Pomeron exchange considered here should contribute (*e.g.* Pomeron loops) and a more general approach for the high density (saturation) regime must be considered. However, we believe that this approach allows us to estimate the magnitude of the high density effects in the kinematical range of the future eA colliders.

In the present work, we shall use two models for the dipole-proton cross section σ_{dp} . One is the very popular GBW model [3], which interpolates between the small and large dipole configurations, providing color transparency behavior, $\sigma_{dp} \sim r^2$, as $r \rightarrow 0$ and constant behavior, $\sigma_{dp} \sim \sigma_0$, at large dipole separation. This model is no longer able to describe the most recent HERA data and it has been replaced by other parameterizations. However we shall keep using it as a baseline, which will be compared with other dipole-proton cross sections, giving us an estimate of the sensitivity of the observable to changes in the dipole cross sections. The parameterization of the dipole-proton cross section is given by the eikonal-like form [3],

$$\sigma_{dp}^{\text{GBW}}(\tilde{x}, \mathbf{r}^2) = \sigma_0 \left[1 - \exp \left(-\frac{Q_s^2(\tilde{x}) \mathbf{r}^2}{4} \right) \right], \quad Q_s^2(\tilde{x}) = \left(\frac{x_0}{\tilde{x}} \right)^\lambda \text{ GeV}^2, \quad (3)$$

where the saturation scale Q_s^2 defines the onset of the saturation phenomenon, which depends on energy, and $\tilde{x} = (Q^2 + 4m_f^2)/(Q^2 + W_{\gamma N}^2)$ (See [3] for details). One of the drawbacks of the GBW model is that it has no impact parameter dependence. It is assumed that the impact parameter dependence of \mathcal{N} can be factorized as $\mathcal{N}(x, \mathbf{r}, \mathbf{b}) = \mathcal{N}(x, \mathbf{r})S(\mathbf{b})$ and this last function is integrated over \mathbf{b} , giving rise to the parameter σ_0 .

During the last years an intense activity in the area resulted in more sophisticated dipole proton cross sections, which had more theoretical constraints and which were able to give a better description of the more recent HERA and/or RHIC data [20, 21, 22, 33, 34, 35, 36]. In what follows we will use the b-CGC model proposed in Ref. [20], which improves the IIM model [6] with the inclusion of the impact parameter dependence in the dipole proton cross sections. The parameters of this model were recently fitted to describe the current HERA data [22]. Following [20] we have that the dipole-proton cross section is given by:

$$\sigma_{dp}^{bCGC}(x, \mathbf{r}^2) \equiv \int d^2\bar{\mathbf{b}} \frac{d\sigma_{dp}}{d^2\bar{\mathbf{b}}} \quad (4)$$

where

$$\frac{d\sigma_{dp}}{d^2\bar{\mathbf{b}}} = 2\mathcal{N}^p(x, \mathbf{r}, \bar{\mathbf{b}}) = 2 \times \begin{cases} \mathcal{N}_0 \left(\frac{rQ_s}{2}\right)^{2\left(\gamma_s + \frac{\ln(2/rQ_s)}{\kappa\lambda Y}\right)} & rQ_s \leq 2 \\ 1 - \exp^{-a \ln^2(b r Q_s)} & rQ_s > 2 \end{cases} \quad (5)$$

with $Y = \ln(1/x)$ and $\kappa = \chi''(\gamma_s)/\chi'(\gamma_s)$, where χ is the LO BFKL characteristic function. The coefficients a and b are determined uniquely from the condition that $\mathcal{N}^p(x, \mathbf{r})$ and its derivative with respect to rQ_s are continuous at $rQ_s = 2$. In this model, the proton saturation scale Q_s now depends on the impact parameter:

$$Q_s \equiv Q_s(x, \bar{\mathbf{b}}) = \left(\frac{x_0}{x}\right)^{\frac{\lambda}{2}} \left[\exp\left(-\frac{\bar{\mathbf{b}}^2}{2B_{CGC}}\right) \right]^{\frac{1}{2\gamma_s}}. \quad (6)$$

The parameter B_{CGC} was adjusted to give a good description of the t -dependence of exclusive J/ψ photoproduction. Moreover the factors \mathcal{N}_0 and γ_s were taken to be free. In this way a very good description of F_2 data was obtained. The parameter set which is going to be used here is the one presented in the second line of Table II of [22]: $\gamma_s = 0.46$, $B_{CGC} = 7.5 \text{ GeV}^{-2}$, $\mathcal{N}_0 = 0.558$, $x_0 = 1.84 \times 10^{-6}$ and $\lambda = 0.119$.

The paper is organized as follows. In next section (Section II) we discuss the coherent and incoherent vector meson production and present our main formulas. In Section III we present our predictions for the energy and Q^2 dependences of the ρ and J/Ψ total cross sections considering the coherent and incoherent cases for two different nuclei. Moreover, we estimate the ratio between the coherent and incoherent cross sections. Finally, in Section IV we summarize our main conclusions.

II. EXCLUSIVE VECTOR MESON PRODUCTION IN THE COLOR DIPOLE APPROACH

In the color dipole approach the exclusive vector meson production ($\gamma^*A \rightarrow VY$) in electron-nucleus interactions at high energies can be factorized in terms of the fluctuation of the virtual photon into a $q\bar{q}$ color dipole, the dipole-nucleus scattering by a color singlet exchange and the recombination into the final state vector meson. This process is characterized by a rapidity gap in the final state. If the nucleus scatters elastically, $Y = A$, the process is called coherent production. On the other hand, if the nucleus scatters inelastically, i. e. breaks up ($Y = X$), the process is denoted incoherent production. In this paper we will consider the color dipole description of the $\gamma^*A \rightarrow VY$ ($V = \rho, J/\Psi$) process, which is quite successful for the proton case [5, 18, 19, 20, 21, 22, 37] and can be extended to nuclei targets with the Glauber-Gribov formalism (For recent reviews see [38, 39]). To a large extent we follow the pioneering papers [40, 41, 42, 43, 44, 45, 46], where these issues were first addressed and also their further developments [47, 48, 49, 50, 51]. To be more precise, in this work we will update the calculations presented in [52], extending them also to electroproduction and treating more carefully the two production mechanisms, coherent and incoherent. For this we shall use the formalism described in detail in Ref. [49]. For the dipole cross section we shall use the parameterization introduced in [22], which was able to give a very good description of data on exclusive vector meson production on proton targets. In this sense our work is an extension of [22] to nuclear targets.

As discussed above, the exclusive vector meson production in electron-nucleus interactions can be classified as coherent or incoherent. If the reaction leaves the target intact, the process is usually called coherent, and the mesons produced at different longitudinal coordinates and impact parameters add up coherently. The corresponding integrated cross section is given in the high energy regime (large coherence length: $l_c \gg R_A$) by [49]

$$\sigma^{coh}(\gamma^*A \rightarrow VA) = \int d^2\bar{\mathbf{b}} \left\{ \left| \int d^2\mathbf{r} \int dz \Psi_V^*(\mathbf{r}, z) \mathcal{N}^A(x, \mathbf{r}, \bar{\mathbf{b}}) \Psi_{\gamma^*}(\mathbf{r}, z, Q^2) \right|^2 \right\} \quad (7)$$

On the other hand, the diffractive incoherent production of vector mesons off nuclei, $\gamma^*A \rightarrow VX$, is associated with the breakup of the nucleus. In this case one sums over all final states of the target nucleus, except those that contain particle production. The t slope is the same as in the case of a nucleon target. Therefore we have:

$$\sigma^{inc}(\gamma^*A \rightarrow VX) = \frac{|\text{Im} \mathcal{A}(s, t=0)|^2}{16\pi B_V} \quad (8)$$

where at high energies ($l_c \gg R_A$) [49]:

$$|\text{Im} \mathcal{A}(s, t=0)|^2 = \int d^2\bar{\mathbf{b}} T_A(\bar{\mathbf{b}}) \left[\left| \int d^2\mathbf{r} \int dz \Psi_V^*(\mathbf{r}, z) \sigma_{dp} \exp\left[-\frac{1}{2} \sigma_{dp} T_A(\bar{\mathbf{b}})\right] \Psi_{\gamma^*}(\mathbf{r}, z, Q^2) \right|^2 \right] \quad (9)$$

$V(m_V)$ (MeV)	m_f (GeV)	R^2 (GeV $^{-2}$)	N_L	N_T	\hat{e}_f
$\rho(776)$	0.14	12.9	0.853	0.911	$1/\sqrt{2}$
$J/\Psi(3097)$	1.4	2.3	0.575	0.578	$2/3$

TABLE I: Parameters and normalization of the boosted-Gaussian overlap function.

The $q\bar{q}$ pair attenuates with a constant absorption cross section, as in the Glauber model, except that the whole exponential is averaged rather than just the cross section in the exponent. The coherent and incoherent cross sections depend differently on t . As discussed in [43], at small- t ($-t R_A^2/3 \ll 1$) coherent production dominates the lepton production of vector mesons, with the signature being a sharp forward diffraction peak. On the other hand, incoherent production will dominate the vector meson production at large- t ($-t R_A^2/3 \gg 1$), with the t -dependence being to a good accuracy the same as in the production off free nucleons. Therefore, it is expected that this signature will allow us to separate the two contributions even at a limited resolution in t . However, at an electron-ion collider, if the nucleus remains intact in a small- t interaction, it will escape too close to the beam to be detectable. This implies that the experimental separation between coherent and incoherent production will be a challenging task. In this paper we focus our study on the energy and Q^2 dependence of the total coherent and incoherent cross sections and their relative weights. We postpone the study of the t -dependence of these cross sections for a future publication.

In the Eqs. (7) and (9) the functions $\Psi_{h,\bar{h}}^\gamma(z, \mathbf{r})$ and $\Psi_{h,\bar{h}}^V(z, \mathbf{r})$ are the light-cone wavefunctions of the photon and vector meson, respectively. The quark and antiquark helicities are labeled by h and \bar{h} and reference to the meson and photon helicities are implicitly understood. The variable \mathbf{r} defines the relative transverse separation of the pair (dipole) and z ($1-z$) is the longitudinal momentum fraction of the quark (antiquark). In the dipole formalism, the light-cone wavefunctions $\Psi_{h,\bar{h}}(z, \mathbf{r})$ in the mixed representation (r, z) are obtained through two dimensional Fourier transform of the momentum space light-cone wavefunctions $\Psi_{h,\bar{h}}(z, \mathbf{k})$ (see more details, e.g. in Ref. [19]). The normalized light-cone wavefunctions of longitudinally (L) and transversely (T) polarized photons are given by [20]:

$$\Psi_{h,\bar{h}}^L(z, \mathbf{r}) = \sqrt{\frac{N_c}{4\pi}} \delta_{h,-\bar{h}} e e_f 2z(1-z) Q \frac{K_0(\varepsilon r)}{2\pi}, \quad (10)$$

$$\Psi_{h,\bar{h}}^{T(\gamma=\pm)}(z, \mathbf{r}) = \pm \sqrt{\frac{N_c}{2\pi}} e e_f [ie^{\pm i\theta_r} (z\delta_{h\pm, \bar{h}\mp} - (1-z)\delta_{h\mp, \bar{h}\pm})\partial_r + m_f \delta_{h\pm, \bar{h}\pm}] \frac{K_0(\varepsilon r)}{2\pi}, \quad (11)$$

where $\varepsilon^2 = z(1-z)Q^2 + m_f^2$. The quark mass m_f plays the role of a regulator when the photoproduction regime is reached. Namely, it prevents non-zero argument for the modified Bessel functions $K_{0,1}(\varepsilon r)$ towards $Q^2 \rightarrow 0$. The electric charge of the quark of flavor f is given by $e e_f$.

For vector mesons, the light-cone wavefunctions are not known in a systematic way and have to be determined in a phenomenological way. Here, we follow the approach proposed in Refs. [45, 46] and discussed in detail in [19, 20, 54]. It is assumed that the spin and polarization of the vector mesons are the same as in the photon, which is considered as being predominantly a quark-antiquark state. Consequently, the wavefunctions for a transversely and longitudinally polarized vector meson are given by

$$\Psi_{h\bar{h}, \lambda=\pm 1}^V(r, z) = \pm \sqrt{\frac{N_c}{2\pi}} \frac{1}{z(1-z)} \{ie^{\pm i\theta_r} [z\delta_{h,\pm}\delta_{\bar{h},\mp} - (1-z)\delta_{h,\mp}\delta_{\bar{h},\pm}]\partial_r + m_f \delta_{h,\pm}\delta_{\bar{h},\pm}\} \phi_T(r, z). \quad (12)$$

and

$$\Psi_{h\bar{h}, \lambda=0}^V(r, z) = \sqrt{\frac{N_c}{2\pi}} \delta_{h,-\bar{h}} \left[M_V + \delta \frac{m_f^2 - \nabla_r^2}{M_V z(1-z)} \right] \phi_L(r, z), \quad (13)$$

where $\nabla_r^2 \equiv (1/r)\partial_r + \partial_r^2$ and M_V is the meson mass. As emphasized in [19], the longitudinally polarized wave function is slightly more complicated due to the fact that the coupling of the quarks to the meson is non-local, contrary to the photon case.

Following Ref. [21] we define the overlap function between the photon and vector meson wave functions by

$$\Phi_\lambda^{\gamma^* V}(z, \mathbf{r}; Q^2, M_V^2) = \sum_{f h \bar{h}} \left[\Psi_{f, h, \bar{h}}^{V, \lambda}(z, \mathbf{r}; M_V^2) \right]^* \Psi_{f, h, \bar{h}}^{\gamma^*, \lambda}(z, \mathbf{r}; Q^2). \quad (14)$$

Using the above expressions for the photon and vector meson wave functions we get (See appendix of Ref. [21]):

$$\Phi_L^{\gamma^*V}(z, \mathbf{r}, Q^2) = \hat{e}_f \sqrt{\frac{\alpha_e}{4\pi}} N_c 2Q K_0(\varepsilon r) \left[M_V z(1-z) \phi_L(\mathbf{r}, z) + \frac{m_f^2 - \nabla_r^2}{M_V} \phi_L(\mathbf{r}, z) \right], \quad (15)$$

$$\Phi_T^{\gamma^*V}(z, \mathbf{r}, Q^2) = \hat{e}_f \sqrt{\frac{\alpha_e}{4\pi}} N_c \frac{\alpha_e N_c}{2\pi^2} \{ m_f^2 K_0(\varepsilon r) \phi_T(r, z) - [z^2 + (1-z)^2] \varepsilon K_1(\varepsilon r) \partial_r \phi_T(r, z) \}, \quad (16)$$

where

$$\phi_{L,T} = N_{L,T} \exp \left[-\frac{m_f^2 R^2}{8z(1-z)} + \frac{m_f^2 R^2}{2} - \frac{2z(1-z)r^2}{R^2} \right]. \quad (17)$$

and the parameters R and $N_{L,T}$ are constrained by unitarity of the wavefunction as well as by the electronic decay widths. The parameters used in our calculations are presented in Table I. Our choice is usually denoted in literature as *boosted Gaussian* (BG) wavefunctions and are a simplified version ($\delta = 1$) of the wavefunctions proposed by Nemchik, Nikolaev, Predazzi and Zakharov in Refs. [45, 46]. We quote Refs. [19, 20, 21] for more details and comparison with data for both photo and electroproduction of vector mesons in ep collisions at HERA.

Using the above expressions for the vector meson wave functions, we obtain

$$|\mathcal{I}m \mathcal{A}_{L,T}|^2 = \int d^2\mathbf{b} T_A(\mathbf{b}) \left\{ \left| \int d^2\mathbf{r} \int dz \Phi_{L,T}^{\gamma^*V}(z, \mathbf{r}, Q^2) \sigma_{dp} \exp\left[-\frac{1}{2}\sigma_{dp} T_A(\mathbf{b})\right] \right|^2 \right\}, \quad (18)$$

and

$$\sigma^{coh}(\gamma_{L,T}^* A \rightarrow VA) = \int d^2\mathbf{b} \left\{ \left| \int d^2\mathbf{r} \int dz \Phi_{L,T}^{\gamma^*V}(z, \mathbf{r}, Q^2) \left[2 \left(1 - \exp\left[-\frac{1}{2}\sigma_{dp} T_A(\mathbf{b})\right] \right) \right] \right|^2 \right\}. \quad (19)$$

In what follows we will estimate the total cross section for the exclusive vector meson production using as input in the Eqs. (18) and (19) the GBW and bCGC parameterizations for the dipole-proton cross section.

III. RESULTS

The project of an electron-ion collider is being elaborated by groups at BNL (eRHIC) [9] and at CERN (LHeC) [55]. The main expectation is that the future eA collider should have a center of mass energy larger than 60 GeV and a high luminosity, such that measurements of inclusive observables at low- x and diffractive processes could be improved substantially. Here we will analyze the energy and Q^2 dependence of the coherent and incoherent total cross section for J/Ψ and ρ vector meson production. We will consider two different nuclei (Ca and Pb) in order to study the A -dependence of our predictions.

Moreover, we will also use as input in our calculations the linear limit of the GBW and bCGC dipole-proton cross section in order to determine the sensitivity of our results to the saturation effects in the proton. In the GBW model we take the linear limit by using instead of σ_{dp} , the expansion of (3) when the dipole is very small ($r \rightarrow 0$) and the exponent is small. In this case $\sigma_{dp} = \sigma_0 \frac{Q_s^2(\bar{x}) r^2}{4}$. In the bCGC model the linear behavior is estimated by taking only the first line of Eq. (5).

Let us start our analysis considering nuclear photoproduction of vector mesons. In Figs. 1 and 2 we present our predictions for the energy dependence of the coherent and incoherent total cross sections, respectively. As expected, the cross section grows with the energy and with the atomic number. We predict huge coherent cross sections, in reasonable agreement with those presented in [52], where a different approach was used to estimate the cross sections. At fixed atomic number, the coherent cross section is approximately a factor 70 (25) larger than the incoherent one for ρ (J/Ψ) photoproduction. Furthermore, at fixed energy, the coherent cross section increases with the atomic number faster than the incoherent one, in agreement with the conclusions from [26].

The photoproduction of ρ in nuclear collisions is a typical soft process, characterized by large dipole pair separations. At high energies, the saturation scale can assume large values and become the hard scale of the problem. The transition between these two regimes is determined by the energy dependence of the saturation scale, which is model dependent. From Figs. 1 and 2 we can see that for the ρ meson the full predictions of the GBW and bCGC models are very similar, in contrast with the linear ones. While the cross sections are strongly dependent on assumptions concerning saturation in the proton in the GBW case, they are very similar when we use the linear and full expressions of the bCGC model. This behavior is directly associated to the large difference between the linear and full expressions in the

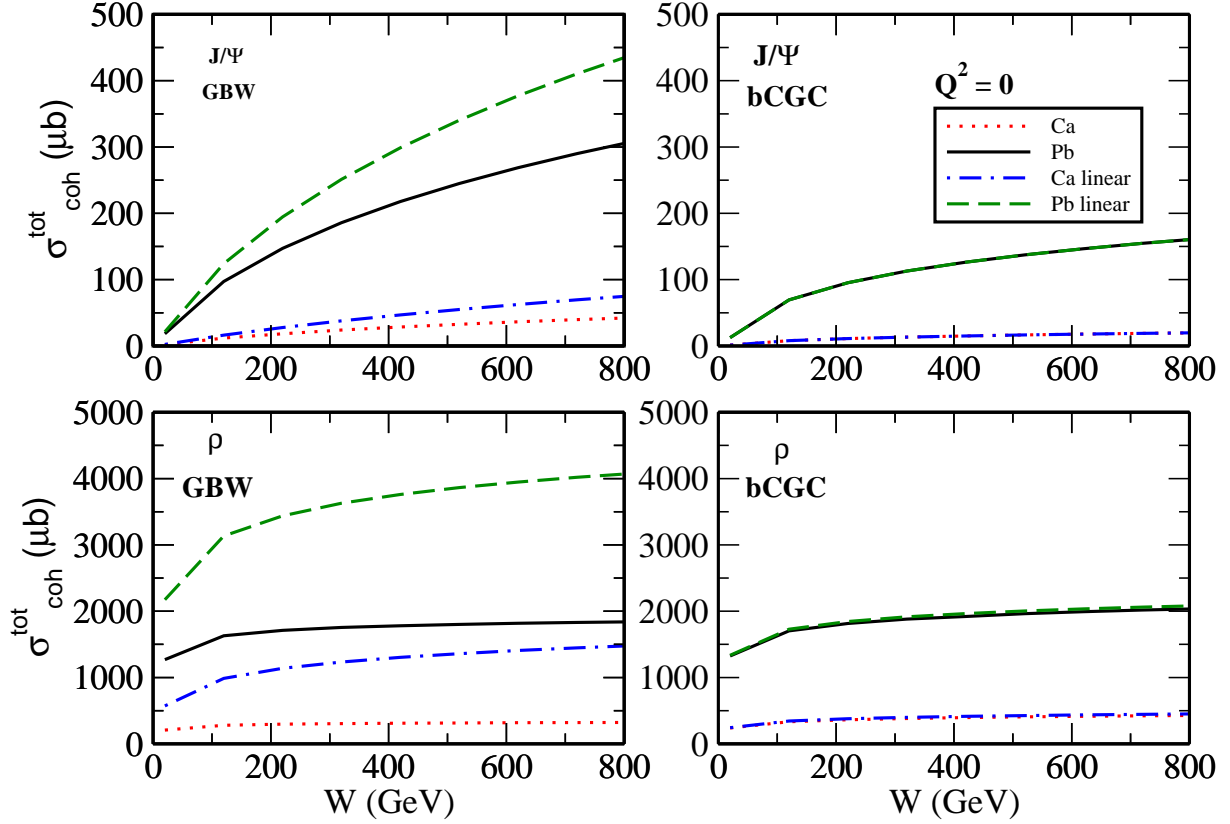


FIG. 1: Coherent photoproduction cross sections for J/ψ and ρ vector meson production with the GBW (left panels) and bCGC (right panels) models.

GBW model at large dipole pair separation, which is smaller in the bCGC model. Concerning J/ψ photoproduction, which is characterized by a hard scale, the mass of J/ψ , the total cross sections increase faster with the energy than in the case of the ρ . Moreover, the GBW and bCGC predictions are very different, which is directly associated with the energy dependence of the saturation scale in these two models. Similarly to the ρ case, the linear and full GBW predictions are different, while are similar when we use the bCGC model.

In Figs. 3 and 4 we present our predictions for the photon virtuality Q^2 dependence of the coherent and incoherent total cross sections, respectively. As expected, the total cross sections decrease with Q^2 . The Q^2 behavior predicted by the GBW and bCGC models are similar. The main difference is associated to the strong dependence on the saturation effects in the proton observed when we use the GBW model. Moreover, the Q^2 dependence of the J/ψ cross section is smaller than the ρ one, which is directly associated to the hard scale present in the J/ψ case.

Finally, in Figs. 5 and 6 we present our predictions for the energy and Q^2 dependences of the ratio between the incoherent and coherent cross sections, respectively. The incoherent contribution is a small fraction of the coherent one and the ratio decreases with the energy. Moreover, the ratio is larger for small values of the atomic number. These conclusions are weakly model dependent. Concerning the Q^2 dependence, the ratio decreases at larger Q^2 , with a stronger dependence in the case of the ρ meson, as expected from the discussion above. It is important to emphasize that at large Q^2 the ratio is larger for J/ψ than for ρ production. We can conclude that although measuring experimentally the intact recoil nucleus (coherent process) in a future electron ion collider may be very difficult, our results strongly suggest that this is the dominant process in vector meson production, specially when we focus on high energy eA reactions. This conclusion agrees with that obtained in [26].

So far we have been working only with two phenomenological models for the dipole-proton scattering amplitude, GBW and bCGC, and one might wonder what would be the results obtained with other existing models. In a previous paper we have performed a more systematic comparison between different dipole models [56]. Based on this comparison, we believe that using other scattering amplitudes would slightly change the normalization of our

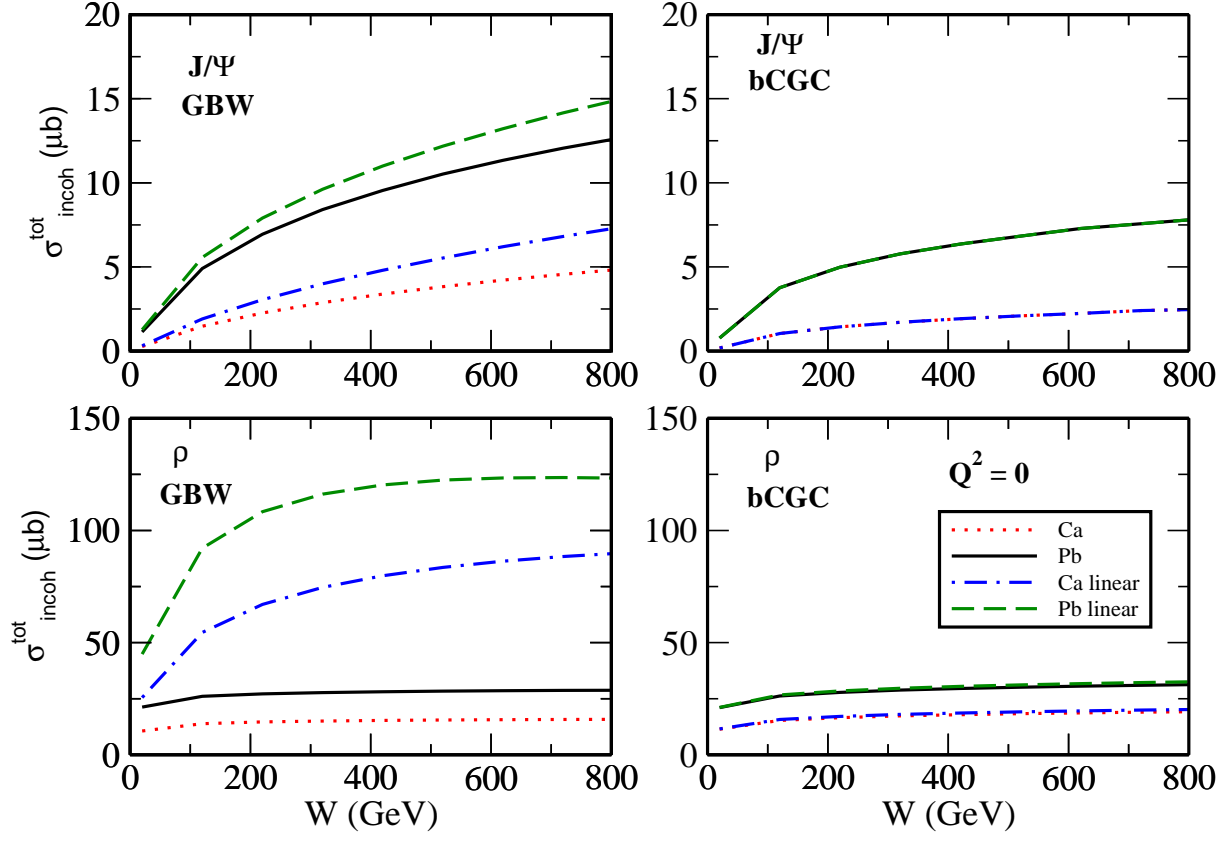


FIG. 2: Incoherent photoproduction cross sections for J/ψ and ρ vector meson production with the GBW (left panels) and bCGC (right panels) models.

predictions for the cross sections. However all the qualitative features would remain the same. In particular the low sensitivity to non-linear effects in the proton, observed in all the curves obtained with the bCGC model, would be the same for the other models. This can be traced back to the dependence of the saturation scale on the energy and dipole pair separation, which determine the speed with which the amplitude goes to one, which is very similar in the modern phenomenological models based on the CGC formalism.

IV. CONCLUSIONS

Although a large body of experimental data has been accumulated by the HERA collaborations H1 and ZEUS over more than one decade in ep collisions, very little is known about vector meson production off nuclei at high energies. In this regime we expect a significant contribution from saturation physics. In this paper we have estimated the coherent and incoherent cross sections for the exclusive vector meson production considering the color dipole approach and phenomenological saturation models which describe the scarce F_2^A data as well as the HERA data. Our results demonstrate that the coherent production of vector mesons is dominant, with a small contribution coming from incoherent processes. Probably in the future eA colliders the separation between coherent and incoherent processes will be difficult. However, in view of our results it might be worth trying.

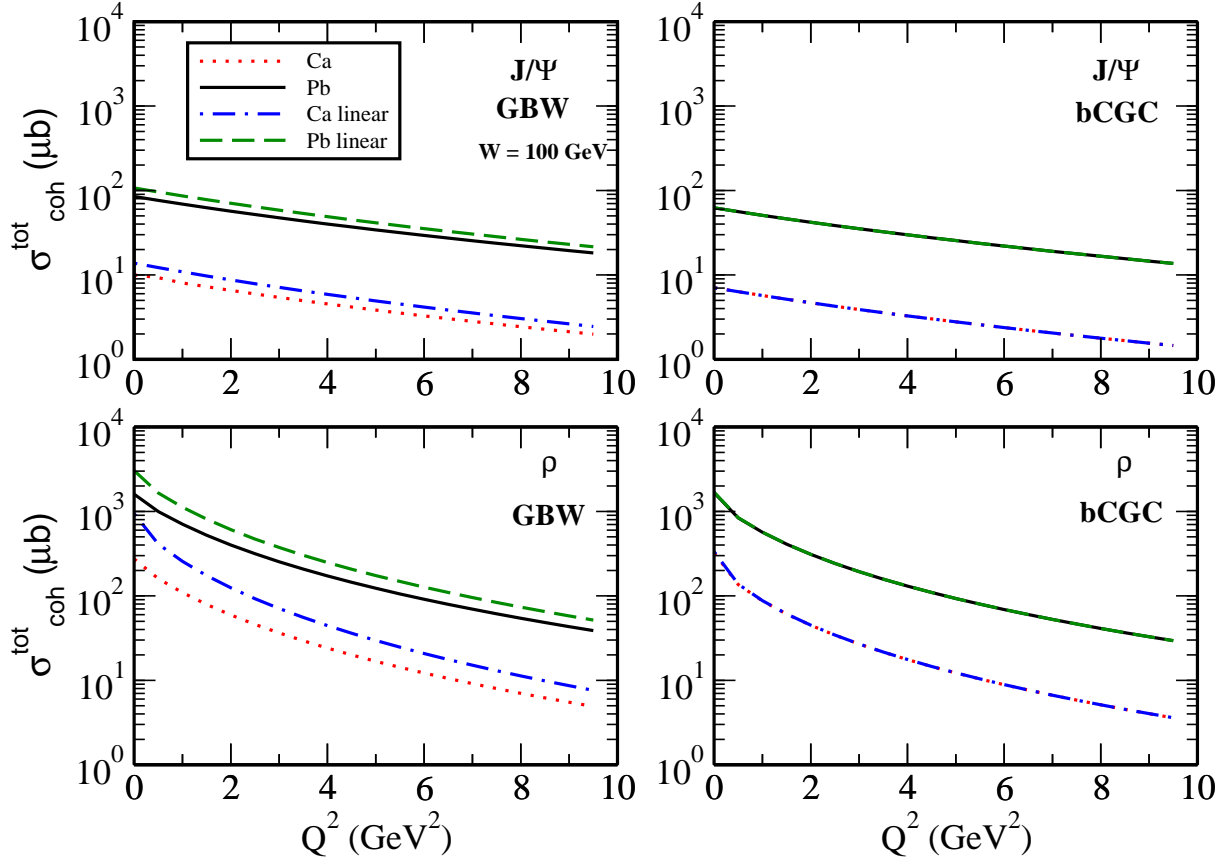


FIG. 3: Coherent electroproduction cross sections for J/ψ and ρ with the GBW (left panels) and bCGC (right panels) models as a function of Q^2 at fixed center of mass energy ($W = 100 \text{ GeV}$).

Acknowledgments

This work was partially financed by the Brazilian funding agencies CNPq and FAPESP. The authors are deeply grateful to M. Munhoz, A.J.R. da Silva and R.G. Amorim for providing access to their computing facilities.

-
- [1] E. Iancu and R. Venugopalan, arXiv:hep-ph/0303204; A. M. Stasto, Acta Phys. Polon. B **35**, 3069 (2004); H. Weigert, Prog. Part. Nucl. Phys. **55**, 461 (2005); J. Jalilian-Marian and Y. V. Kovchegov, Prog. Part. Nucl. Phys. **56**, 104 (2006).
 - [2] E. Gotsman, E. Levin, M. Lublinsky and U. Maor, Eur. Phys. J. C **27**, 411 (2003).
 - [3] K. Golec-Biernat and M. Wüsthoff, Phys. Rev. D **59**, 014017 (1999), *ibid.* D **60**, 114023 (1999).
 - [4] J. Bartels, K. Golec-Biernat, H. Kowalski, Phys. Rev. D **66**, 014001 (2002).
 - [5] H. Kowalski and D. Teaney, Phys. Rev. D **68**, 114005 (2003).
 - [6] E. Iancu, K. Itakura, S. Munier, Phys. Lett. B **590**, 199 (2004).
 - [7] J. R. Forshaw and G. Shaw, JHEP **0412**, 052 (2004).
 - [8] R. Venugopalan, AIP Conf. Proc. **588**, 121 (2001). [arXiv:hep-ph/0102087].
 - [9] A. Deshpande, R. Milner, R. Venugopalan and W. Vogelsang, Ann. Rev. Nucl. Part. Sci. **55**, 165 (2005).
 - [10] M. S. Kugeratski, V. P. Goncalves and F. S. Navarra, Eur. Phys. J. C **46**, 413 (2006).
 - [11] M. S. Kugeratski, V. P. Goncalves and F. S. Navarra, Eur. Phys. J. C **46**, 465 (2006).
 - [12] E. R. Cazaroto, F. Carvalho, V. P. Goncalves and F. S. Navarra, Phys. Lett. B **669**, 331 (2008).
 - [13] E. R. Cazaroto, F. Carvalho, V. P. Goncalves and F. S. Navarra, Phys. Lett. B **671**, 233 (2009).

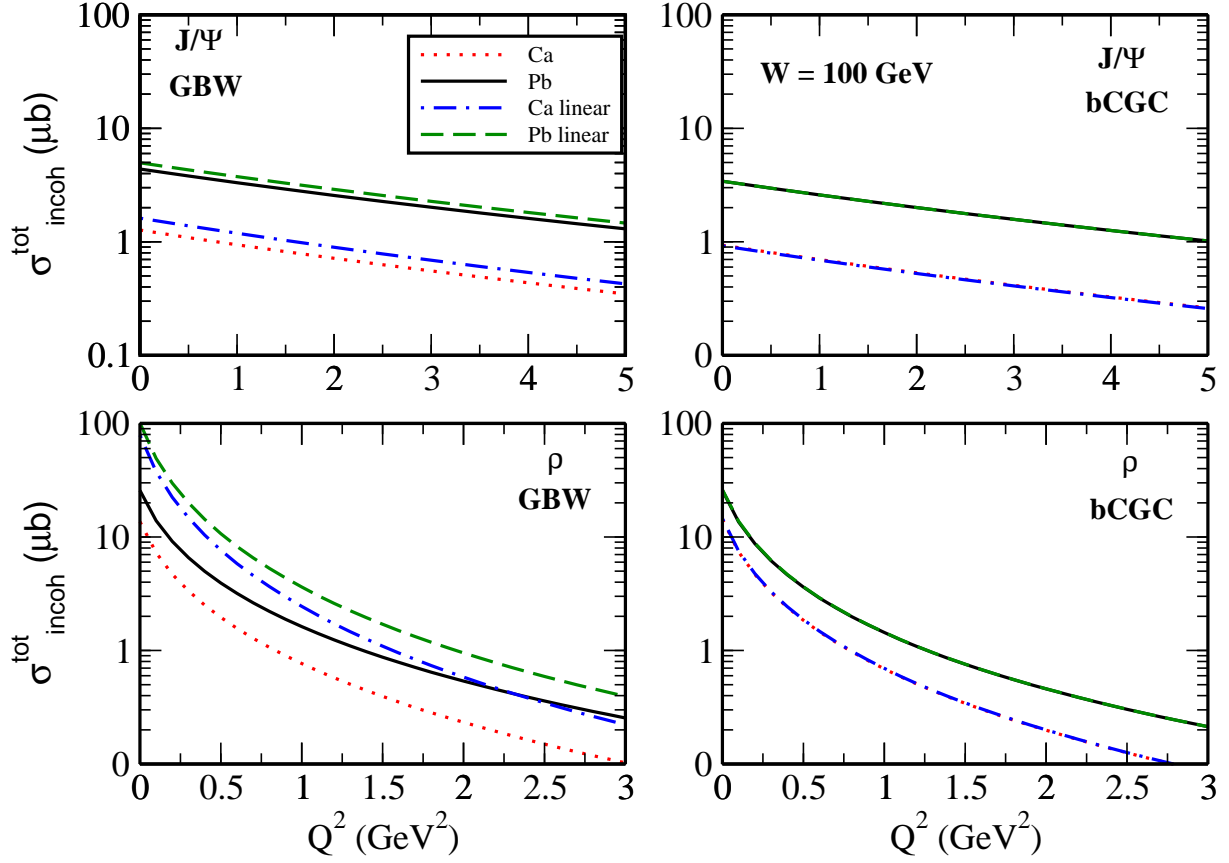


FIG. 4: Incoherent electroproduction cross sections for J/ψ and ρ with the GBW (left panels) and bCGC (right panels) models as a function of Q^2 at fixed center of mass energy ($W = 100$ GeV).

- [14] H. Kowalski, T. Lappi and R. Venugopalan, Phys. Rev. Lett. **100**, 022303 (2008) .
- [15] H. Kowalski, T. Lappi, C. Marquet and R. Venugopalan, Phys. Rev. C **78**, 045201 (2008).
- [16] N. N. Nikolaev, W. Schafer, B. G. Zakharov and V. R. Zoller, JETP Lett. **84**, 537 (2007)
- [17] N. N. Nikolaev, B. G. Zakharov and V. R. Zoller, Z. Phys. A **351**, 435 (1995).
- [18] A. C. Caldwell and M. S. Soares, Nucl. Phys. A **696**, 125 (2001).
- [19] J. R. Forshaw, R. Sandapen and G. Shaw, Phys. Rev. D **69**, 094013 (2004).
- [20] H. Kowalski, L. Motyka and G. Watt, Phys. Rev. D **74**, 074016 (2006).
- [21] C. Marquet, R. B. Peschanski and G. Soyez, Phys. Rev. D **76**, 034011 (2007)
- [22] G. Watt and H. Kowalski, Phys. Rev. D **78**, 014016 (2008).
- [23] Y. Li and K. Tuchin, Phys. Rev. D **77**, 114012 (2008)
- [24] Y. Li and K. Tuchin, Nucl. Phys. A **807**, 190 (2008)
- [25] Y. Li and K. Tuchin, Phys. Rev. C **78**, 024905 (2008)
- [26] K. Tuchin, arXiv:0812.1519 [hep-ph].
- [27] F. Dominguez, C. Marquet and B. Wu, arXiv:0812.3878 [nucl-th].
- [28] J. L. Albacete, Phys. Rev. Lett. **99**, 262301 (2007).
- [29] J. L. Albacete, N. Armesto, J. G. Milhano and C. A. Salgado, arXiv:0902.1112 [hep-ph].
- [30] N. Armesto, Eur. Phys. J. C **26**, 35 (2002).
- [31] V. P. Goncalves and M. V. T. Machado, Eur. Phys. J. C **30**, 387 (2003).
- [32] V. N. Gribov, Sov. Phys. JETP **29**, 483 (1969); Sov. Phys. JETP **30**, 709 (1970).
- [33] D. Kharzeev, Y.V. Kovchegov and K. Tuchin, Phys. Lett. **B599**, 23 (2004).
- [34] A. Dumitru, A. Hayashigaki and J. Jalilian-Marian, Nucl. Phys. **A765**, 464 (2006); Nucl.Phys. **A770**, 57 (2006).
- [35] V. P. Goncalves, M. S. Kugeratski, M. V. T. Machado and F. S. Navarra, Phys. Lett. B **643**, 273 (2006).
- [36] D. Boer, A. Utermann and E. Wessels, Phys. Rev. D **77**, 054014 (2008).

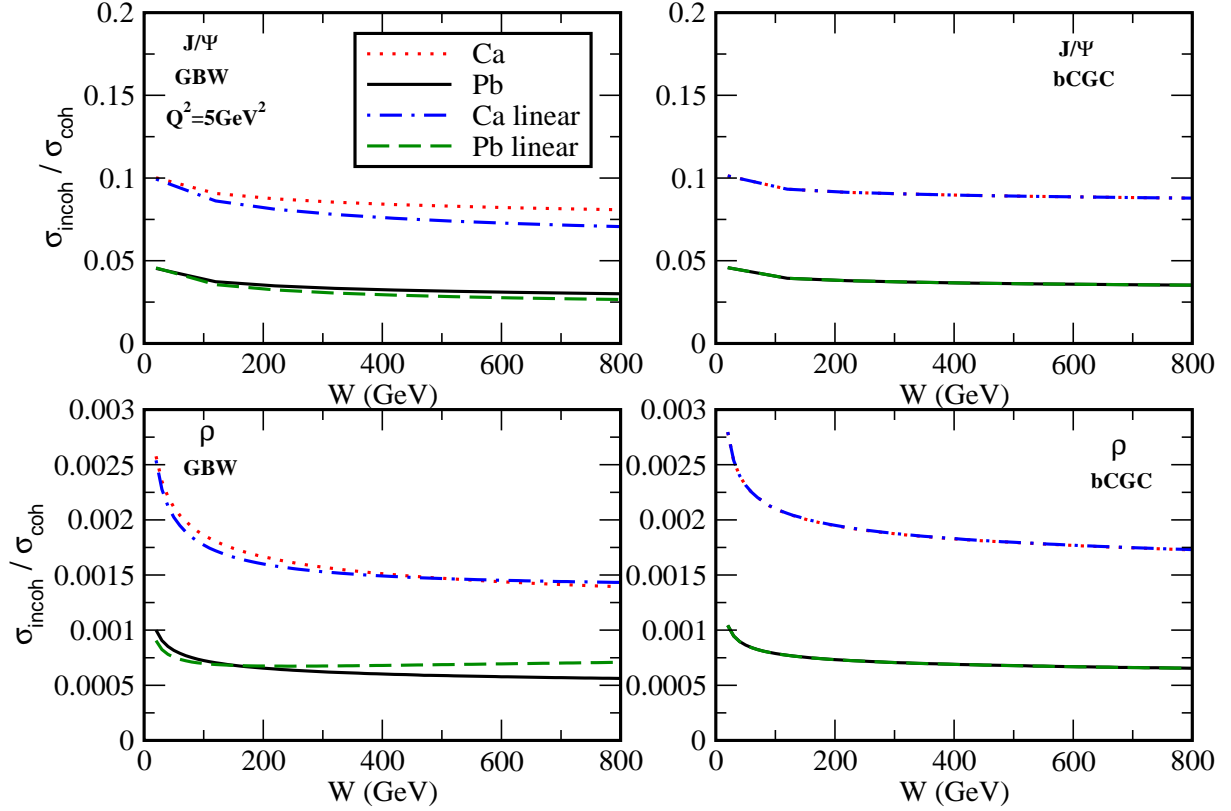


FIG. 5: Ratio $\sigma_{incoherent}/\sigma_{coherent}$ for the nuclear electroproduction of vector mesons as a function of the energy with the GBW (left panels) and bCGC (right panels) models at fixed virtuality ($Q^2 = 5 \text{ GeV}^2$).

- [37] J. Hufner, Yu. P. Ivanov, B. Z. Kopeliovich and A. V. Tarasov, Phys. Rev. D **62** (2000) 094022
- [38] I. P. Ivanov, N. N. Nikolaev and A. A. Savin, Phys. Part. Nucl. **37**, 1 (2006)
- [39] I. P. Ivanov, Acta Phys. Polon. B **39**, 2373 (2008).
- [40] N. N. Nikolaev, Comments Nucl. Part. Phys. **21** (1992) 41.
- [41] O. Benhar, B. Z. Kopeliovich, C. Mariotti, N. N. Nikolaev and B. G. Zakharov, Phys. Rev. Lett. **69** (1992) 1156.
- [42] B. Z. Kopeliovich, J. Nemchik, N. N. Nikolaev and B. G. Zakharov, Phys. Lett. B **309** (1993) 179.
- [43] B. Z. Kopeliovich, J. Nemchik, N. N. Nikolaev and B. G. Zakharov, Phys. Lett. B **324** (1994) 469.
- [44] J. Nemchik, N. N. Nikolaev and B. G. Zakharov, Phys. Lett. B **339** (1994) 194.
- [45] J. Nemchik, N. N. Nikolaev, E. Predazzi and B. G. Zakharov, Phys. Lett. B **374**, 199 (1996)
- [46] J. Nemchik, N. N. Nikolaev, E. Predazzi and B. G. Zakharov, Z. Phys. C **75**, 71 (1997)
- [47] N. N. Nikolaev, J. Speth and B. G. Zakharov, Phys. Atom. Nucl. **63** (2000) 1463 [Yad. Fiz. **63** (2000) 1463].
- [48] O. Benhar, S. Fantoni, N. N. Nikolaev and B. G. Zakharov, J. Exp. Theor. Phys. **84** (1997) 421 [Zh. Eksp. Teor. Fiz. **111** (1997) 769].
- [49] B. Z. Kopeliovich, J. Nemchik, A. Schafer and A. V. Tarasov, Phys. Rev. C **65** (2002) 035201
- [50] Yu. P. Ivanov, B. Z. Kopeliovich, A. V. Tarasov and J. Hufner, Phys. Rev. C **66** (2002) 024903
- [51] B. Z. Kopeliovich, J. Nemchik and I. Schmidt, Phys. Rev. C **76** (2007) 025210
- [52] V. P. Goncalves and M. V. T. Machado, Eur. Phys. J. C **38**, 319 (2004).
- [53] N. N. Nikolaev, B. G. Zakharov, Phys. Lett. B **332**, 184 (1994); Z. Phys. C **64**, 631 (1994).
- [54] H. G. Dosch, T. Gousset, G. Kulzinger and H. J. Pirner, Phys. Rev. **D55**, 2602 (1997).
- [55] J. B. Dainton, M. Klein, P. Newman, E. Perez and F. Willeke, JINST **1**, P10001 (2006).
- [56] M. S. Kugeratski, V. P. Goncalves and F. S. Navarra, Eur. Phys. J. C **44**, 577 (2005).

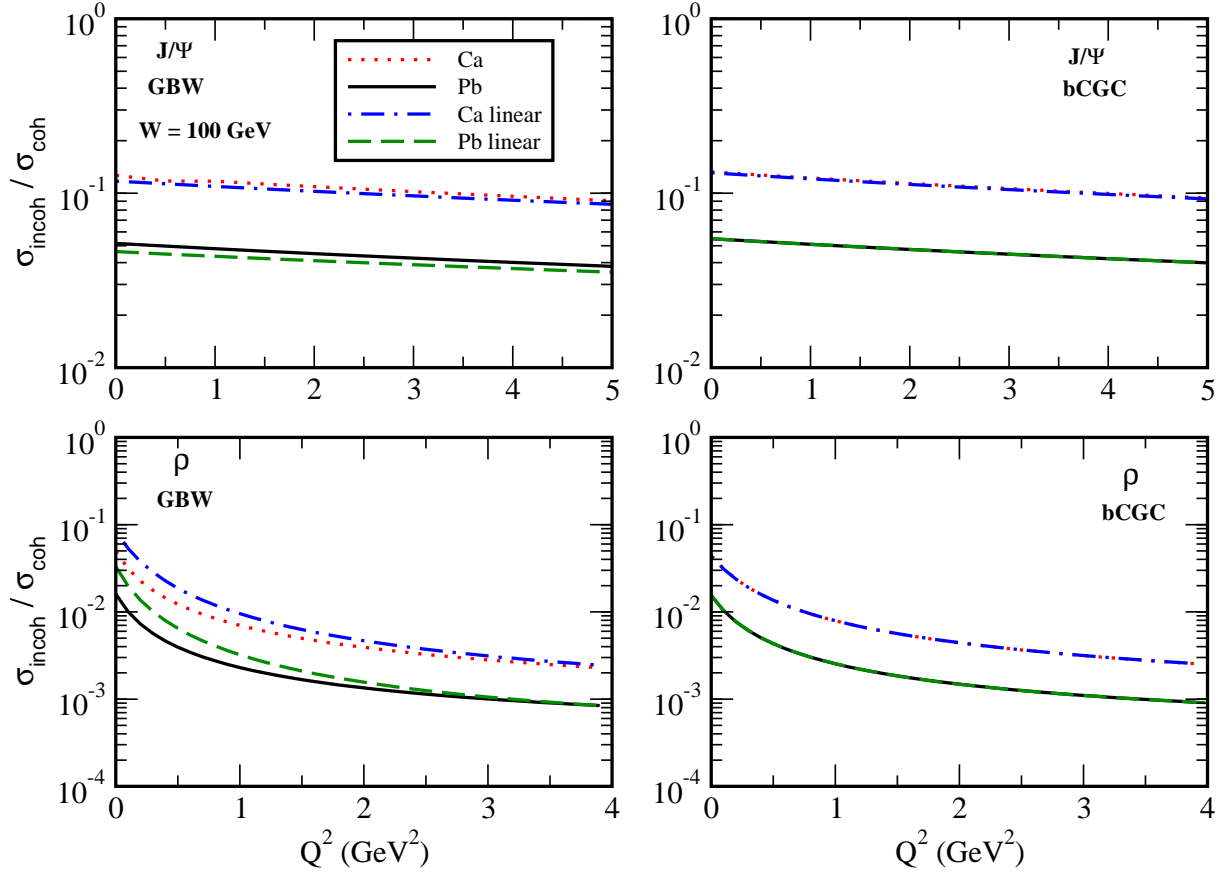


FIG. 6: Ratio $\sigma_{\text{incoherent}}/\sigma_{\text{coherent}}$ for the nuclear electroproduction of vector mesons as a function of the photon virtuality with the GBW (left panels) and bCGC (right panels) models at fixed energy ($W = 100$ GeV).